

Probing the Steric Limits of Carbon–Gold Bond Formation: (Dialkylbiarylphosphine)gold(I) Aryls

David V. Partyka,[‡] James B. Updegraff III,[‡] Matthias Zeller,[†] Allen D. Hunter,[†] and Thomas G. Gray^{*,‡}

Department of Chemistry, Case Western Reserve University, Cleveland, Ohio 44106, and Department of Chemistry, Youngstown State University, 1 University Plaza, Youngstown, Ohio 44555

Received August 1, 2008

Aryl-group transfer from arylboronic acids to gold has emerged as a functionally tolerant alternative to classical lithiation- and magnesiation-based synthesis of arylgold(I) species. Here, the scope of the reaction is explored with attention to the sterics of the boronic acid starting material and the supporting ligand on gold. Dicyclohexylbiaryl phosphines are selected as supporting ligands on gold(I) because of their substantial bulk. Aryl-group transfer is compatible with steric buildup on either reaction partner. The structural preference of gold(I) for linear, two-coordinate geometries circumvents potential steric clashes. The new organometallics likely gain added stability through dative interactions with the flanking phosphine biaryl arm and, in three cases, through π -interactions with the aryl ligand σ -bonded to gold. The new compounds are characterized by multinuclear NMR and optical spectroscopy, X-ray diffraction crystallography, and combustion analysis. All compounds absorb ultraviolet light at wavelengths $\lambda < 325$ nm. Time-dependent density-functional theory calculations find that multiple singlet–singlet transitions account for the absorption profile, which has both intraligand and (ligand–metal)-to-ligand charge-transfer character.

Introduction

Organogold chemistry^{1–4} is undergoing an impressive resurgence for its photophysical dimensions,^{5–13} for cancer therapy and imaging,^{14–19} and not least for its catalytic applicability. The (phosphine)gold(I) fragment and (N-heterocyclic carbene)

analogues, which are isolobal with the proton,^{20–22} catalyze a variety of reactions at unsaturated carbon centers. In broad categories, these include nucleophilic additions across carbon–carbon multiple bonds; activations of alcohols, carbonyl groups, and carbon monoxide; and oxidation reactions.^{23–27} Gold(I) is given to linear two-coordination, and the supporting ligands of choice have been organophosphines and N-heterocyclic carbenes, although phosphites,²⁸ chelating nitrogen donors,²⁹ and other ligands³⁰ have also been employed.

In a number of these studies, steric girth about the supporting ligand has been found to promote catalysis. For example, Echavarren and co-workers³¹ have recently reported 1,3-enyne and arylalkyne [4+2] cycloaddition reactions catalyzed by cationic gold(I) species bearing hindered ligands. Sterically imposing ligands were chosen in part because aryl-substituted

* Corresponding author. E-mail: tgray@case.edu.

[†] Case Western Reserve University.

[‡] Youngstown State University.

(1) Schmidbaur, H.; Schier, A. In *Comprehensive Organometallic Chemistry III*; Crabtree, R., Migos, M., Eds.; Elsevier: New York, 2006; Vol. 2, Section 2.05.

(2) Schmidbaur, H. In *Gmelin Handbuch der Anorganischen Chemie*, 8th ed.; Slawisch, A., Ed.; Springer-Verlag: Berlin, 1980.

(3) Schmidbaur, H.; Grohmann, A.; Olmos, M. E. In *Gold: Progress in Chemistry, Biochemistry and Technology*; Schmidbaur, H., Ed.; Wiley: Chichester, 1999.

(4) Fernández, E. J.; Laguna, A.; Olmos, M. E. *Adv. Organomet. Chem.* **2004**, *52*, 77–141.

(5) Gray, T. G. *Comments Inorg. Chem.* **2007**, *28*, 181–212.

(6) Balch, A. L. *Struct. Bonding (Berlin)* **2007**, *123*, 1–40.

(7) Fackler, J. P., Jr. *Inorg. Chem. Rev.* **2002**, *41*, 6959–6972.

(8) Vickery, J. C.; Olmstead, M. M.; Fung, E. Y.; Balch, A. L. *Angew. Chem., Int. Ed. Engl.* **1997**, *36*, 1179–1181.

(9) Elbjeirami, O.; Omary, M. A.; Stender, M.; Balch, A. L. *Dalton Trans.* **2004**, 3173–3175.

(10) Balch, A. L. *Gold Bull.* **2004**, *37*, 45–50.

(11) Omary, M. A.; Mohamed, A. A.; Rawashdeh-Omary, M. A.; Fackler, J. P., Jr. *Coord. Chem. Rev.* **2005**, *249*, 1372–1381.

(12) Arvapally, R. K.; Sinha, P.; Hettiarachchi, S. R.; Coker, N. L.; Bedel, C. E.; Patterson, H. H.; Elder, R. C.; Wilson, A. K.; Omary, M. A. *J. Phys. Chem. C* **2007**, *111*, 10689–10699.

(13) Elbjeirami, O.; Omary, M. A. *J. Am. Chem. Soc.* **2007**, *129*, 11384–11393.

(14) Barnard, P. J.; Berners-Price, S. J. *Coord. Chem. Rev.* **2007**, *251*, 1889–1902.

(15) Tiekink, E. R. T. *Gold Bull.* **2003**, *36*, 117–124.

(16) Rigobello, M. P.; Scutari, G.; Boscolo, R.; Bindoli, A. *Br. J. Pharmacol.* **2002**, *136*, 1162–1168.

(17) McKeage, M. J. *Br. J. Pharmacol.* **2002**, *136*, 1081–1082.

(18) Ray, S.; Mohan, R.; Singh, J. K.; Samantaray, M. K.; Shaikh, M. M.; Panda, D.; Ghosh, P. *J. Am. Chem. Soc.* **2007**, *129*, 15042–15053.

(19) Barnard, P.; Wedlock, L. E.; Baker, M. V.; Berners-Price, S. J.; Joyce, D. A.; Skelton, B. W.; Steer, J. H. *Angew. Chem., Int. Ed.* **2006**, *45*, 5966–5970.

(20) Hoffmann, R. *Angew. Chem., Int. Ed. Engl.* **1982**, *21*, 711–724.

(21) Hall, K. P.; Mingos, D. M. P. *Prog. Inorg. Chem.* **1984**, *32*, 237–325.

(22) Pyykkö, P. *Angew. Chem., Int. Ed.* **2004**, *43*, 4412–4456.

(23) Gorin, D. J.; Toste, F. D. *Nature* **2007**, *446*, 395–403.

(24) Hashmi, A. S. K. *Chem. Rev.* **2007**, *107*, 3180–3211.

(25) Hashmi, A. S. K.; Hutchings, G. J. *Angew. Chem., Int. Ed.* **2006**, *45*, 7896–7936.

(26) Fürstner, A.; Davies, P. W. *Angew. Chem., Int. Ed.* **2007**, *46*, 3410–3449.

(27) Jiménez-Núñez, E.; Echavarren, A. M. *Chem. Commun.* **2007**, 333–346.

(28) López, S.; Herrero-Gómez, E.; Pérez-Galán, C.; Nieto-Oberhuber, C.; Echavarren, A. M. *Angew. Chem., Int. Ed.* **2006**, *45*, 6029–6032.

(29) Guan, B.; Xing, D.; Cai, G.; Wan, X.; Yu, N.; Fang, Z.; Yang, L.; Shi, Z. *J. Am. Chem. Soc.* **2005**, *127*, 18004–18005.

(30) Teles, J. H.; Brode, S.; Chabanas, M. *Angew. Chem., Int. Ed.* **1998**, *37*, 1415–1418.

(31) Nieto-Oberhuber, C.; Pérez-Galán, P.; Herrero-Gómez, E.; Lauterbach, T.; Rodríguez, C.; López, S.; Bour, C.; Rosellón, A.; Cárdenas, D. J.; Echavarren, A. M. *J. Am. Chem. Soc.* **2008**, *130*, 269–279.

alkynes undergo alkoxycyclization and cycloisomerization reactions with difficulty. Among the most active gold(I) catalysts are complexes having bulky N-heterocyclic carbene ligands and tris(2,6-di-*tert*-butyl)phosphite. In earlier work, the same group³² examined a diverse assortment of hindered phosphines as supporting ligands in the gold(I)-catalyzed cyclization of enynes. Here also, steric heft was necessary for efficient reaction. Bender and Widenhoefer³³ identified a hindered (N-heterocyclic carbene)gold(I) cation, generated by halide abstraction from the chloro complex with Ag⁺, as an active catalyst in the intramolecular hydroamination of *N*-alkenyl ureas. The carbene ligand confers a higher catalytic activity than a similar complex bearing a dialkylbiarylphosphine ligand. Nolan and co-workers³⁴ report a bulky (N-heterocyclic carbene)gold(I) complex to be the catalyst of choice for an indene synthesis. Arguably steric and electronic effects combine in the case of [(*p*-CF₃-C₆H₄)₃P]AuCl, which exceeds other gold(I) precursors in catalyzing the ring expansion of propargyl cyclopropanols.³⁵

Frequently, supporting phosphine ligands deriving from palladium-catalyzed cross-coupling chemistry are applied to investigations of gold(I). The *ortho*-biaryl phosphines of Buchwald and collaborators were originally developed for enhanced reactivity of palladium in Suzuki–Miyaura cross-coupling^{36,37} and other reactions.^{38–45} These ligands are believed to stabilize low-coordinate palladium intermediates, and thereby suppress catalyst decomposition. Recent structural and theoretical studies have examined dative interactions between palladium and the flanking aryl group of the phosphine.^{46–50} X-ray diffraction crystallography studies^{51,52} indicate similar π -interactions in neutral and cationic gold(I) species.

Reported here are synthetic, structural, and spectroscopic studies of (dialkylbiarylphosphine)gold(I) aryl complexes. The compounds herein were prepared in base-induced arylation reactions of the corresponding gold(I) bromides with boronic

acids. The new protocol's tolerance of steric hindrance, on both the (phosphine)gold(I) fragment and the organic transmetalating partner, is emphasized. Products have been characterized by multinuclear NMR, mass spectrometry, elemental analysis, and X-ray diffraction crystallography. Dative interactions between gold(I) and one or two carbon atoms of the flanking aryl moiety are observed in the solid state. Excited-state properties of the new compounds are interrogated with absorption and time-resolved emission spectroscopy. Assignments of optical transitions are made with the use of time-dependent density-functional theory. A portion of this work has been communicated previously.⁵³

Experimental Section

All solvents and reagents were used as received. Microanalyses (C, H, and N) were performed by Quantitative Technologies Inc., Whitehouse, NJ. NMR spectra (¹H, ³¹P) were recorded on a Varian AS-400 spectrometer. UV–visible spectra were recorded on a Cary 5g UV–vis–NIR spectrophotometer. All UV–visible spectra were similar, with a shoulder around the THF solvent cutoff (280 nm) that tails off into the visible region, so all spectra report the molar absorptivity at this wavelength at concentrations in the range (2–6) × 10^{−5} M. Emission spectra were recorded (on a Cary Eclipse fluorescence spectrometer) after solutions had been degassed with argon for at least 20 min.

[(PCy₂(2-biphenyl))Au(phenyl)], 4. In 5 mL of 2-propanol were suspended Cs₂CO₃ (107 mg, 0.33 mmol) and phenylboronic acid (39 mg, 0.32 mmol). To this suspension was added [(PCy₂(2-biphenyl))AuBr] (100 mg, 0.16 mmol), and the resultant mixture was stirred at 50 °C for 30 h. After cooling, the mixture was stripped of solvent in vacuo, extracted into benzene, and filtered through Celite. The filtrate was taken to dryness and triturated with pentane until a white solid formed, which was scraped into the pentane. The pentane was decanted, the solid was extracted into benzene and concentrated to saturation, and pentane was diffused into the saturated solution. A colorless crystalline mass separated, which was washed with cold methanol and pentane, dried, and collected. Yield: 84 mg (84%). ¹H NMR (C₆D₆): δ 7.81–7.86 (m, 2H, C₆H₅), 7.51–7.56 (m, 1H, C₆H₅), 7.49 (td, 2H, C₆H₅, *J* = 1.6, 6.0 Hz), 7.17–7.28 (m, 6H, Cy₂P(C₁₂H₉)), 7.00–7.08 (m, 3H, Cy₂P(C₁₂H₉)), 0.82–2.00 (m, 22H, (C₆H₁₁)₂P(2-biphenyl)) ppm. ³¹P NMR (C₆D₆): δ 50.7 ppm. UV–vis (THF): λ (ϵ , M^{−1} cm^{−1}) 280 (6300) nm. Anal. Calcd for C₃₀H₃₆AuP: C, 57.69; H, 5.81. Found: C, 57.56; H, 5.76.

[(PCy₂(2-biphenyl))Au(2-biphenyl)], 5. In 5 mL of 2-propanol were suspended Cs₂CO₃ (150 mg, 0.46 mmol) and 2-biphenylboronic acid (96 mg, 0.48 mmol). To this suspension was added [(PCy₂(2-biphenyl))AuBr] (144 mg, 0.23 mmol), and the mixture was stirred at 50 °C for 30 h. After cooling, the mixture was stripped of solvent in vacuo, extracted into benzene, filtered through Celite, and taken to dryness by rotary evaporation. Pentane was added to and thoroughly mixed with the white solid and removed via rotary evaporation. The solid was dried, extracted into benzene, and filtered through Celite. Slow evaporation gave colorless crystals; the crystals were ground in and triturated with pentane. The pentane was decanted, and the microcrystalline powder was washed with cold methanol and pentane and dried. Yield: 145 mg (90%). ¹H NMR (C₆D₆): δ 7.91 (dd, 2H, CH, *J* = 1.6, 8.0 Hz), 7.84–7.88 (m, 1H, CH), 7.66 (dt, 1H, CH, *J* = 1.2, 8.0 Hz), 7.58–7.64 (m, 1H, CH), 7.48 (tt, 1H, CH, *J* = 1.2, 7.6 Hz), 7.24–7.30 (m, 3H, CH), 7.12–7.19 (m, 5H, CH), 7.00–7.12 (m, 4H, CH), 0.85–1.86 (m, 22H, C₆H₁₁). ³¹P NMR (C₆D₆): δ 52.8 ppm. UV–vis (THF): λ (ϵ , M^{−1} cm^{−1}) 280 (7710) nm. Anal. Calcd for C₃₆H₄₀AuP: C, 61.71; H, 5.75. Found: C, 61.73; H, 5.72.

(53) Partyka, D. V.; Zeller, M.; Hunter, A. G.; Gray, T. G. *Angew. Chem., Int. Ed.* **2006**, *45*, 8188–8191.

- (32) Muñoz, M. P.; Adrio, J.; Carretero, J. C.; Echavarren, A. M. *Organometallics* **2005**, *24*, 1293–1300.
- (33) Bender, C. F.; Widenhoefer, R. A. *Org. Lett.* **2006**, *8*, 5303–5305.
- (34) Marion, N.; Díez-González, S.; de Frémont, P.; Noble, A. R.; Nolan, S. P. *Angew. Chem., Int. Ed.* **2006**, *45*, 3647–3650.
- (35) Markham, J. P.; Staben, S. T.; Toste, F. D. *J. Am. Chem. Soc.* **2005**, *127*, 9708–9709.
- (36) Old, D. W.; Wolfe, J. P.; Buchwald, S. L. *J. Am. Chem. Soc.* **1998**, *120*, 9722–9723.
- (37) Altman, R. A.; Buchwald, S. L. *Nat. Protoc.* **2007**, *2*, 3115–3121.
- (38) Wolfe, J. P.; Tomori, H.; Sadighi, J. P.; Yin, J.; Buchwald, S. L. *J. Org. Chem.* **2000**, *65*, 1158–1174.
- (39) Anderson, K. W.; Tundel, R. E.; Ikawa, T.; Altman, R. A.; Buchwald, S. L. *Angew. Chem., Int. Ed.* **2006**, *45*, 6523–6527.
- (40) Nguyen, H. N.; Huang, X.; Buchwald, S. L. *J. Am. Chem. Soc.* **2003**, *125*, 11818–11819.
- (41) Walker, S. D.; Barder, T. E.; Martinelli, J. R.; Buchwald, S. L. *Angew. Chem., Int. Ed.* **2004**, *43*, 1871–1876.
- (42) Barder, T. E.; Buchwald, S. L. *Org. Lett.* **2004**, *6*, 2649–2652.
- (43) Billingsley, K.; Buchwald, S. L. *J. Am. Chem. Soc.* **2007**, *129*, 3358–3366.
- (44) Anderson, K. W.; Buchwald, S. L. *Angew. Chem., Int. Ed.* **2005**, *44*, 6173–6177.
- (45) Ikawa, T.; Barder, T. E.; Biscoe, M. R.; Buchwald, S. L. *J. Am. Chem. Soc.* **2007**, *129*, 13001–13007.
- (46) Barder, T. E.; Walker, S. D.; Martinelli, J. R.; Buchwald, S. L. *J. Am. Chem. Soc.* **2005**, *127*, 4685–4696.
- (47) Yin, J.; Rainka, M. P.; Zhang, X.-X.; Buchwald, S. L. *J. Am. Chem. Soc.* **2002**, *124*, 1162–1163.
- (48) Reid, S. M.; Boyle, R. C.; Mague, J. T.; Fink, M. J. *J. Am. Chem. Soc.* **2003**, *125*, 7816–7817.
- (49) Christmann, U.; Vilar, R.; White, A. J. P.; Williams, D. J. *Chem. Commun.* **2004**, 1294–1295.
- (50) Barder, T. E. *J. Am. Chem. Soc.* **2006**, *128*, 898–904.
- (51) Partyka, D. V.; Robilotto, T. J.; Zeller, M.; Hunter, A. D.; Gray, T. G. *Organometallics* **2007**, *26*, 3279–3282.
- (52) Herrero-Gómez, E.; Nieto-Oberhuber, C.; López, S.; Benet-Buchholz, J.; Echavarren, A. M. *Angew. Chem., Int. Ed.* **2006**, *45*, 5455–5459.

[(PCy₂(2'-methylbiphenyl))Au(phenyl)], 6. In 5 mL of 2-propanol were suspended Cs₂CO₃ (95 mg, 0.29 mmol) and phenylboronic acid (39 mg, 0.32 mmol). To this suspension was added [(PCy₂(2'-methylbiphenyl))AuBr] (94 mg, 0.15 mmol), and the mixture was stirred at 50 °C for 30 h. After cooling, the mixture was stripped of solvent in vacuo, extracted into benzene (~20 mL), filtered through Celite, and washed thoroughly with ethylene glycol (3 × 8 mL) and water (2 × 10 mL). The organic layer was separated and dried with MgSO₄, filtered, and taken to a residue via rotary evaporation. Pentane was added, thoroughly mixed, and removed via rotary evaporation; this process was repeated. The sticky white solid was extracted again into benzene, filtered, and taken to a residue by rotary evaporation. Pentane was added, thoroughly mixed, and removed via rotary evaporation; this process was repeated. The white solid was collected and dried. Yield: 68 mg (63%). ¹H NMR (C₆D₆): δ 7.74–7.79 (m, 2H, C₆H₅), (td, 1H, C₆H₅, *J* = 1.2, 8.8 Hz), 7.11–7.28 (m, 6H, CH), 7.00–7.06 (m, 2H, CH), 6.93–6.98 (m, 1H, CH), 2.09 (s, 3H, CH₃), 0.97–2.08 (m, 22H, C₆H₁₁). ³¹P NMR (C₆D₆): δ 46.3 ppm. UV–vis (THF): λ (ε, M⁻¹ cm⁻¹) 280 (6450) nm. Anal. Calcd for C₃₁H₃₈AuP: C, 58.31; H, 6.00. Found: C, 57.95; H, 6.01.

[(PCy₂(2'-methylbiphenyl))Au(2-biphenyl)], 7. In 5 mL of 2-propanol were suspended Cs₂CO₃ (102 mg, 0.31 mmol) and 2-biphenylboronic acid (62 mg, 0.31 mmol). To this suspension was added [(PCy₂(2'-methylbiphenyl))AuBr] (95 mg, 0.15 mmol), and the mixture was stirred at 50 °C for 30 h. After cooling, the mixture was stripped of solvent by rotary evaporation, extracted into benzene (~20 mL), and filtered through Celite. The benzene solution was washed with ethylene glycol (3 × 10 mL) and water (2 × 10 mL), dried with MgSO₄, filtered, and concentrated by rotary evaporation to a residue. Pentane was added to the residue, and the residue was allowed to sit until crystals formed. The crystals were collected, and the remaining pentane was concentrated by rotary evaporation until a residue remained again. Pentane was added and the mixture stored in a freezer to yield a second crop of crystals. Yield: 65 mg (71%). ¹H NMR (C₆D₆): δ 7.86 (dd, 2H, CH, *J* = 1.2, 8.4 Hz), 7.70–7.74 (m, 1H, CH), 7.63 (dt, 1H, CH, *J* = 1.2, 8.0 Hz), 7.47 (tt, 1H, CH, *J* = 1.6, 8.4 Hz), 7.21–7.30 (m, 4H, CH), 7.15–7.19 (m, 1H, CH), 6.91–7.14 (m, 7H, CH), 2.00 (s, 3H, CH₃), 0.81–2.08 (m, 22H, C₆H₁₁). ³¹P NMR (C₆D₆): δ 46.1 ppm. UV–vis (THF): λ (ε, M⁻¹ cm⁻¹) 280 (8350) nm. Anal. Calcd for C₃₆H₄₀AuP: C, 62.18; H, 5.92. Found: C, 62.26; H, 5.63.

[(PCy₂(2'-methylbiphenyl))Au(mesityl)], 8. To 6 mL of 2-propanol were added mesitylboronic acid (80 mg, 0.49 mmol) and Cs₂CO₃ (134 mg, 0.41 mmol). To this suspension was added [(PCy₂(2'-methylbiphenyl))AuBr] (104 mg, 0.16 mmol), and the resultant mixture was stirred for 60 h at 50 °C. After cooling, the mixture was stripped of solvent via rotary evaporation, extracted into benzene, filtered through Celite, washed with ethylene glycol (3 × 10 mL), washed with water (2 × 10 mL), and dried with MgSO₄. After filtration, the solution was taken to a residue via rotary evaporation, triturated with pentane, and rotovapped to a residue (the product slowly dissolves in pentane over time). The residue was re-extracted into benzene, cooled to ~0 °C, and filtered again. The same pentane trituration procedure, repeated twice, yielded a white solid, which had to be recrystallized (pentane/benzene) to give an analytically pure material. Yield: 50 mg (45%). ¹H NMR (C₆D₆): δ 7.34–7.40 (m, 1H, 2'-methylbiphenyl), 6.92–7.13 (m, 9H, 2'-methylbiphenyl + C₆H₂(CH₃)₃), 2.74 (s, 6H, C₆H₂(CH₃)₃), 2.39 (s, 3H, C₆H₂(CH₃)₃), 2.08 (s, 3H, 2'-methylbiphenyl), 0.84–2.26 (m, 22H, C₆H₁₁). ³¹P NMR (C₆D₆): δ 48.1 ppm. UV–vis (THF): λ (ε, M⁻¹ cm⁻¹) 280 (6910) nm. Anal. Calcd for C₃₄H₄₄AuP: C, 60.00; H, 6.52. Found: C, 60.11; H, 6.67.

[(XPhos)Au(phenyl)], 9. In 5 mL of 2-propanol were suspended Cs₂CO₃ (109 mg, 0.33 mmol) and phenylboronic acid (41 mg, 0.34 mmol). To this suspension was added [(XPhos)AuBr] (112 mg, 0.15 mmol), and the mixture was stirred at 50 °C for 30 h. After

cooling, the mixture was stripped of solvent in vacuo, extracted into benzene, filtered, and taken to dryness in vacuo. The solid was washed with pentane and dried, re-extracted into benzene, filtered, and concentrated to saturation, and pentane vapor was diffused. The flaky white crystals that separated were washed with cold methanol and pentane and dried. Yield: 83 mg (74%). ¹H NMR (C₆D₆): δ 7.60–7.64 (m, 2H, C₆H₅), 7.40 (td, 2H, C₆H₅, *J* = 1.2, 8.0 Hz), 7.24 (s, 2H, XPhos), 7.11–7.22 (m, 3H, XPhos), 6.98–7.04 (m, 2H, Cy₂P(2',4',6'-(Prⁱ)₃(C₁₂H₆))), 2.82 (sep, 1H, CH(CH₃)₂, *J* = 7.2 Hz), 2.56 (sep, 2H, CH(CH₃)₂, *J* = 6.8 Hz), 1.57 (d, 6H, CH(CH₃)₂, *J* = 7.2 Hz), 1.17 (d, 6H, CH(CH₃)₂, *J* = 7.2 Hz), 1.08 (d, 6H, CH(CH₃)₂, *J* = 7.2 Hz), 0.91–2.02 (m, 22H, C₆H₁₁). ³¹P NMR (C₆D₆): δ 43.7 ppm. UV–vis (THF): λ (ε, M⁻¹ cm⁻¹) 280 (4170) nm. Anal. Calcd for C₃₉H₅₄AuP: C, 62.31; H, 7.37. Found: C, 62.30; H, 7.28.

[(XPhos)Au(2-biphenyl)], 10. In 5 mL of 2-propanol were suspended Cs₂CO₃ (115 mg, 0.35 mmol) and 2-biphenylboronic acid (74 mg, 0.37 mmol). To this suspension was added [(XPhos)AuBr] (133 mg, 0.18 mmol), and the mixture was stirred at 50 °C for 30 h. After cooling, the mixture was stripped of solvent in vacuo, extracted into benzene, filtered through Celite, and taken to dryness in vacuo. The white solid was washed thoroughly with pentane, dried, extracted into benzene, and filtered through Celite. Slow evaporation gave wet-looking colorless crystals; the crystals were ground in and triturated with pentane. The pentane was decanted, and the microcrystalline powder was washed with cold methanol and pentane and dried. Yield: 116 mg (80%). ¹H NMR (C₆D₆): δ 7.79 (dd, 2H, CH, *J* = 1.2, 8.0 Hz), 7.62–7.68 (m, 1H, CH), 7.52 (d, 1H, CH, *J* = 7.6 Hz), 7.44 (tt, 1H, CH, *J* = 1.2, 8.0 Hz), 7.30 (t, 2H, CH, *J* = 8.0 Hz), 7.23 (s, 2H, CH), 7.14–7.22 (m, 4H, CH), 6.98–7.05 (m, 2H, CH), 2.78 (sep, 1H, (CH₃)₂CH, *J* = 7.2 Hz), 2.51 (sep, 2H, (CH₃)₂CH, *J* = 6.8 Hz), 1.47 (d, 6H, (CH₃)₂CH, *J* = 6.8 Hz), 1.12 (d, 6H, (CH₃)₂CH, *J* = 6.8 Hz), 1.06 (d, 6H, (CH₃)₂CH, *J* = 7.2 Hz), 0.94–1.94 (m, 22H, C₆H₁₁). ³¹P NMR (C₆D₆): δ 42.8 ppm. UV–vis (THF): λ (ε, M⁻¹ cm⁻¹) 280 (8730) nm. Anal. Calcd for C₄₅H₅₈AuP: C, 65.36; H, 7.07. Found: C, 64.98; H, 7.12.

[(XPhos)Au(mesityl)], 11. In 5 mL of 2-propanol were suspended Cs₂CO₃ (118 mg, 0.36 mmol) and mesitylboronic acid (83 mg, 0.51 mmol). To this suspension was added [(XPhos)AuBr] (114 mg, 0.15 mmol), and the mixture was stirred at 55 °C for 60 h. After cooling, the mixture was stripped of solvent in vacuo, extracted into ~20 mL of benzene, and filtered through Celite. The benzene layer was washed three times with 10 mL of ethylene glycol and twice with water (10 mL). After drying with MgSO₄, the benzene layer was filtered through Celite and taken to dryness by rotary evaporation. Pentane was added to and thoroughly mixed with the residue, and the pentane was removed with rotary evaporation. The solid was extracted again into benzene, filtered, and taken to dryness via rotary evaporation. Pentane was added and subsequently removed by rotary evaporation to dry the microcrystalline solid, which was collected. Yield: 104 mg (87%). ¹H NMR (C₆D₆): δ 7.14–7.25 (m, 2H, XPhos), 7.19 (s, 2H, XPhos), 7.06 (s, 2H, C₆H₂(CH₃)₃), 7.01–7.05 (m, 2H, XPhos), 2.75 (sep, 1H, (CH₃)₂CH), 2.69 (s, 6H, C₆H₂(CH₃)₃), 2.59 (sep, 2H, (CH₃)₂CH), 2.35 (s, 3H, C₆H₂(CH₃)₃), 1.56 (d, 6H, (CH₃)₂CH), 1.12 (d, 6H, (CH₃)₂CH), 1.05 (d, 6H, (CH₃)₂CH), 1.00–2.15 (m, 22H, C₆H₁₁). ³¹P NMR (C₆D₆): δ 44.2 ppm. UV–vis (THF): λ (ε, M⁻¹ cm⁻¹) 280 (6510) nm. Anal. Calcd for C₄₂H₆₀AuP: C, 63.79; H, 7.39. Found: C, 63.51; H, 7.68.

Computations. Spin-restricted density-functional theory computations were performed within the Gaussian 03 program suite.⁵⁴ Calculations employed the modified Perdew–Wang exchange

(54) Frisch, M. J.; et al. *Gaussian 03, Revision D.01*; Gaussian, Inc.: Wallingford, CT, 2004.

functional of Adamo and Barone⁵⁵ and the original Perdew–Wang correlation functional.⁵⁶ Nonmetal atoms were described with the TZVP basis set of Godbelt, Andzelm, and co-workers.⁵⁷ Gold orbitals were described with the Stuttgart effective core potential and the associated basis set,⁵⁸ which was contracted as follows: Au, (8s,7p,6d)→[6s,5p,3d]. Relativity with the Stuttgart ECP and its associated basis set is introduced with a potential term (i.e., a one-electron operator) that replaces the two-electron exchange and Coulomb operators resulting from interaction between core electrons and between core and valence electrons. In this way relativistic effects, especially scalar effects, are included implicitly rather than as four-component, one-electron functions in the Dirac equation. We have previously found this combination of functional and basis set to yield satisfactory comparisons with experiment.^{51,53,59} Test computations run with the same basis and other functional yielded qualitatively similar results. The geometries of **4** and **5** are those of the crystal structures, except that hydrogen-atom positions were optimized using the 6-31G(d,p) basis set on nonmetal atoms (gold was treated with the Stuttgart ECP and basis).⁶⁰ Vertical excitation energies were calculated using a TDDFT implementation described by Scuseria and co-workers.⁶¹ All calculated properties reported here include implicit THF solvation ($\epsilon = 7.58$, 298.15 K), which was incorporated in single-point calculations of the gas-phase geometries with Tomasi's polarizable continuum model (PCM). The stability of each converged density was confirmed by calculation of the eigenvalues of the *A* matrix.^{62,63} Percentage compositions of molecular orbitals, overlap populations, and bond orders between fragments were calculated using the AOMix program.^{64,65}

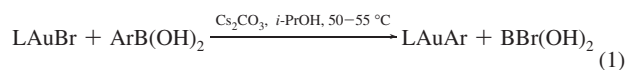
X-ray Structure Determinations. All new products were crystallized by diffusion of pentane into saturated benzene solutions. Single-crystal X-ray data were collected on a Bruker AXS SMART APEX or APEX II CCD diffractometer using monochromatic Mo K α radiation with omega scan technique. The unit cells were determined using SMART⁶⁶ and SAINT+. Data collection for all crystals was conducted at 100 K (−173.5 °C). All structures were solved by direct methods and refined by full matrix least-squares against *F*² with all reflections using SHELXTL.⁶⁸ All non-hydrogen atoms were refined anisotropically. All hydrogen atoms were placed in standard calculated positions, and all hydrogen atoms were refined with an isotropic displacement parameter 1.5 (methyl) or 1.2 times (all others) that of the adjacent carbon.

- (55) Adamo, C.; Barone, V. *J. Chem. Phys.* **1998**, *108*, 664–675.
 (56) Perdew, J. P.; Wang, Y. *Phys. Rev. B* **1992**, *45*, 13244–13249.
 (57) Godbout, N.; Salahub, D. R.; Andzelm, J.; Wimmer, E. *Can. J. Chem.* **1992**, *70*, 560–571.
 (58) Dolg, M.; Wedig, U.; Stoll, H.; Preuss, H. *J. Chem. Phys.* **1987**, *86*, 866–872.
 (59) Partyka, D. V.; Robilotto, T. J.; Zeller, M.; Hunter, A. D.; Gray, T. G. *Proc. Natl. Acad. Sci., U.S.A.* **2008**, *105*, 14293–14297.
 (60) (a) Hariharan, P. C.; Pople, J. A. *Theor. Chim. Acta* **1973**, *28*, 213–222. (b) Franci, M. M.; Pietro, W. J.; Hehre, W. J.; Binkley, J. S.; Gordon, M. S.; DeFrees, D. J.; Pople, J. A. *J. Chem. Phys.* **1982**, *77*, 3654–3665. (c) Clark, T.; Chandrasekhar, J.; Spitznagel, G. W.; Schleyer, P. v. R. *J. Comput. Chem.* **1983**, *4*, 294–301. (d) Krishnam, R.; Binkley, J. S.; Seeger, R.; Pople, J. A. *J. Chem. Phys.* **1980**, *72*, 650. (e) Gill, P. M. W.; Johnson, B. G.; Pople, J. A.; Frisch, M. J. *Chem. Phys. Lett.* **1992**, *197*, 499–505.
 (61) Stratman, R. E.; Scuseria, G. E.; Frisch, M. J. *J. Chem. Phys.* **1998**, *109*, 8218–8224.
 (62) Seeger, R.; Pople, J. A. *J. Chem. Phys.* **1977**, *66*, 3045–3050.
 (63) Bauernschmitt, R.; Alrichs, R. *J. Chem. Phys.* **1996**, *104*, 9047–9052.
 (64) Gorelsky, S. I. *AOMix: Program for Molecular Orbital Analysis*; York University: Toronto, 1997; <http://www.sg-chem.net>.
 (65) Gorelsky, S. I.; Lever, A. B. P. *J. Organomet. Chem.* **2001**, *635*, 187–196.
 (66) *SMART for WNT/2000* (Version 5.628), Bruker Advanced X-ray Solutions; Bruker AXS Inc.: Madison, WI, 1997–2002.
 (67) *SAINT* (Version 6.45), Bruker Advanced X-ray Solutions; Bruker AXS Inc.: Madison, WI, 1997–2003.
 (68) *SHELXTL* (Version 6.10), Bruker Advanced X-ray Solutions; Bruker AXS Inc.: Madison, WI, 2000.

Results and Discussion

Syntheses. Much previous organogold(I) chemistry predicates on organolithium or Grignard reagents.^{1–4} In these instances, (phosphine)- or (N-heterocyclic carbene)gold(I) halides transmetalate upon reaction with formal carbanions to produce the corresponding arylgold(I) species and the corresponding lithium or magnesium halides. These protocols can suffer from the limited functional group tolerance of *s*-block organometallics, although noteworthy progress has followed the low-temperature synthesis of functionalized organomagnesium reagents.⁶⁹

Recently, we have disclosed a milder, functionally tolerant means of arylgold(I) synthesis. (Phosphine)- or (N-heterocyclic carbene)gold(I) bromides are reacted with arylboronic acids or esters in alcohol solvents at 50–55 °C in the presence of a base, eq 1.⁵³



L = PR₃, N-heterocyclic carbene; Ar = aryl group

Cesium carbonate provides the best results. Arylation also occurs in the presence of cesium fluoride, but in lower yields. An attempted arylation reaction done with sodium carbonate did not yield organogold product. Cesium carbonate is more soluble in isopropyl alcohol at 50 °C than either CsF or Na₂CO₃; this greater solubility may account for the higher yields of gold(I) aryls. Aryl-group transfer here proceeds from boron to gold in comparable or better yields, and in shorter time spans, than with Grignard reagents at room temperature. Earlier investigations by Fackler,⁷⁰ Schmidbaur,⁷¹ and their respective co-workers found phenyl-group transfer from BPh₄[−] to gold(I) under similarly mild conditions. Arylation from boron tolerates the reducible and polar functional groups that react with formally carbanionic reagents. The method employs only reagents and yields only products that, when pure, are stable indefinitely to air and moisture. We find the new method to be remarkably forgiving of bulk: steric buildup in the (phosphine)gold(I) halide, the boronic acid, or both affords crowded organogold products in uncompromised yields.

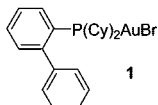
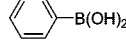
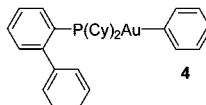
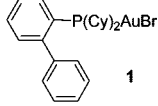
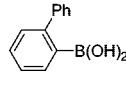
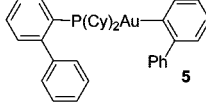
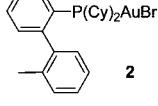
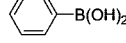
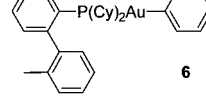
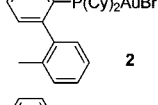
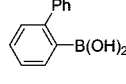
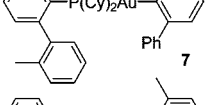
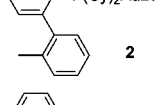
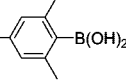
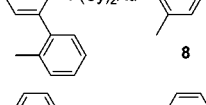
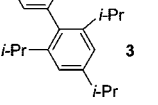
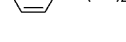
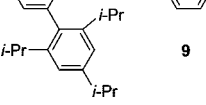
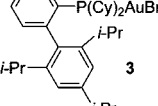
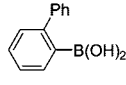
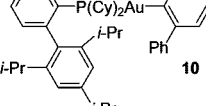
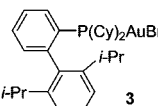
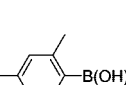
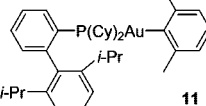
The dialkylbiarylphosphines of Buchwald and collaborators^{36–50} were selected as accessible (commercially obtainable) extremes of steric encumbrance. Table 1 collects bromogold(I) starting materials and the organometallic products derived from them; a numbering system is indicated. The compounds are isolated as white solids upon trituration of benzene solutions with pentane in yields ranging from 45 to 90%.

Reaction times that afford optimal yields vary from 30–60 h and are similar to or somewhat longer than those for (tricyclohexylphosphine)- or (N-heterocyclic carbene)gold(I) products. None of the new compounds show any sensitivity to air, moisture, or ambient light over a period of months in the solid state.

Phosphorus-31 NMR spectroscopy diagnoses aryl group transfer to gold. Whereas ³¹P NMR resonances of the bromide starting materials fall between 36.0 and 46.0 ppm, those of the corresponding aryls are downfield-shifted. For the complexes in Table 1, the range of ³¹P chemical shifts is 42.8 ppm (**10**) to

- (69) Knochel, P.; Dohle, W.; Gommermann, N.; Kneisel, F. F.; Kopp, F.; Korn, T.; Sapountzis, I.; Vu, V. A. *Angew. Chem., Int. Ed.* **2003**, *42*, 4302–4320.
 (70) Forward, J. M.; Fackler, J. P., Jr.; Staples, R. J. *Organometallics* **1995**, *14*, 4194–4198.
 (71) Sladek, A.; Hofreiter, S.; Paul, M.; Schmidbaur, H. *J. Organomet. Chem.* **1995**, *501*, 47–51.

Table 1. (Phosphine)gold(I) Reactants, Products, and Isolated Yields

Gold(I) precursor	Arylboronic acid	Product	Isolated yield
			84%
			90%
			63%
			71%
			45%
			74%
			80%
			87%

52.8 ppm (**5**). In all cases, the ^{31}P NMR resonances shift downfield 4.7–7.5 ppm from those of the starting bromide upon arylation. This observation concurs with previous reports of the sensitivity of bound-phosphorus resonances to the *trans*-situated ligand opposite gold.^{72,73} ^1H NMR resonances of the phosphine ligands are relatively insensitive to metal arylation.

Structures. All new organogold products have been crystallographically characterized. Table 2 collects crystallographic data. Figure 1 depicts thermal ellipsoid plots of two representatives, **5** and **11**. In no structure are auriphilic contacts (gold–gold separations ≤ 3.6 Å^{74–76}) observed.

Table 3 compiles selected interatomic distances and angles. Au–P bond lengths are similar to those encountered elsewhere.^{77–79} Au–C σ -bond lengths range from 2.022(7) Å for one crystallographically independent molecule of **10** to 2.065(2)

Å for **11**. As observed in gold(I) halide complexes,^{51,80} dative interactions join gold to the *ipso* and *ortho* carbon atoms of the flanking biaryl moieties bound to phosphorus. Au–C_{*ipso*} separations range from 3.171(7) Å for one independent molecule of **10** to 3.357(6) Å for one independent molecule of **6**; the sum of the van der Waals radii for gold and carbon is 3.36 Å.⁸¹ The corresponding range of Au–C_{*ortho*} distances, where C_{*ortho*} is the nearer biarylphosphine *ortho* carbon, is 3.225(3) Å (for **9**) to 3.462(6) Å for one crystallographically unique molecule of **6**. In four instances, a phosphine *ortho* carbon is nearer gold than the neighboring *ipso* center: in **4** and **9** and in one independent molecule each of **6** and **10**.

Some years ago, Kochi and co-workers⁸² proposed a geometric criterion of hapticity η^x that holds for atoms binding asymmetrically across a carbon–carbon multiple bond:

$$x = 1 + 2 \frac{\sqrt{d_1^2 - D^2}}{\sqrt{d_1^2 - D^2} + \sqrt{d_2^2 - D^2}} \quad (2)$$

In this expression, D is the length of a normal vector that extends from gold to the best-fit plane of the six pendant aryl-ring carbons, and d_1 and d_2 are the nearest and second-nearest Au–C distances, respectively ($d_1 \leq d_2$). Table 4 collects hapticity values x calculated this way; they range from 1.41 for one crystallographically independent molecule of **10** to 1.93 for the other independent molecule of **10**. These values should be increased by 1 if binding of the σ -carbon is to be included. The mean hapticity is 1.67. However, in two instances a third biphenylphosphine carbon penetrates within van der Waals contact (≤ 3.36 Å) of gold: in **7** and **8**. For these, the hapticity of the phosphine biphenyl arm may more accurately be said to exceed 2.

All gold centers approach a linear P–Au–C _{σ -aryl} geometry. The corresponding bond angles centered about gold range from 169.13(16)° in one independent molecule of **6** to 175.85(17)° in one molecule of **10**.

The three compounds (**5**, **7**, and **10**) bearing *o*-biphenyl ligands present additional gold–carbon π -interactions. Table 5 summarizes salient interatomic distances. In compound **5**, gold approaches the biphenyl ligand *ipso* carbon more closely [3.289(2) Å] than any carbon of the flanking biphenyl substituent of the phosphine ligand. In the structures of **7** and **10**, similar dative interactions with the σ -biphenyl ligand occur, but all biphenyl ligand carbons are more distant from gold than the *ipso* carbons of the phosphine ligands. In **5**, **7**, and **10**, the *ortho* carbon of the σ -biaryl ligand approaches within bonding reach of gold. No evidence for aryl or benzylic carbon–hydrogen bond activation has been found among the new compounds.⁸⁴

Optical Spectroscopy. The new organometallics are colorless or off-white solids, in common with their bromide precursors.

(79) Baenziger, N. C.; Bennett, W. E.; Soboroff, D. M. *Acta Crystallogr., Sect. B* **1976**, 32, 962–963.

(80) Herrero-Gómez, E.; Nieto-Oberhuber, C.; López, S.; Benet-Buchholz, J.; Echavarren, A. M. *Angew. Chem., Int. Ed.* **2006**, 45, 5455–5459.

(81) Bondi, A. J. *J. Phys. Chem.* **1964**, 68, 441–451.

(82) Vasilyev, A. V.; Lindeman, S. V.; Kochi, J. K. *Chem. Commun.* **2001**, 909–910.

(83) Kochi hapticities for the flanking phenyls of these σ -biphenyl ligands bound directly to gold all hover near $x = 1.96$. However, the chemical significance of these values is doubtful. The side-on phenyl groups are forced into greater proximity than for the flanking phosphine phenyls. Therefore D in eq 1 ranges from 2.1 to 2.7. For phosphine biaryls, D falls between 3.1 and 3.3. The Kochi hapticities for the phenyl groups of the C-bound biphenyls are somewhat artificially compressed about $x = 2$, and skepticism about their meanings appears in order.

(72) Baker, L.-J.; Bott, R. C.; Bowmaker, G. A.; Healy, P. C.; Skelton, B. W.; Schwerdtfeger, P.; White, A. H. *J. Chem. Soc., Dalton Trans.* **1995**, 1341–1347.

(73) Bott, R. C.; Healy, P. C.; Smith, G. *Polyhedron* **2007**, 26, 2803–2809.

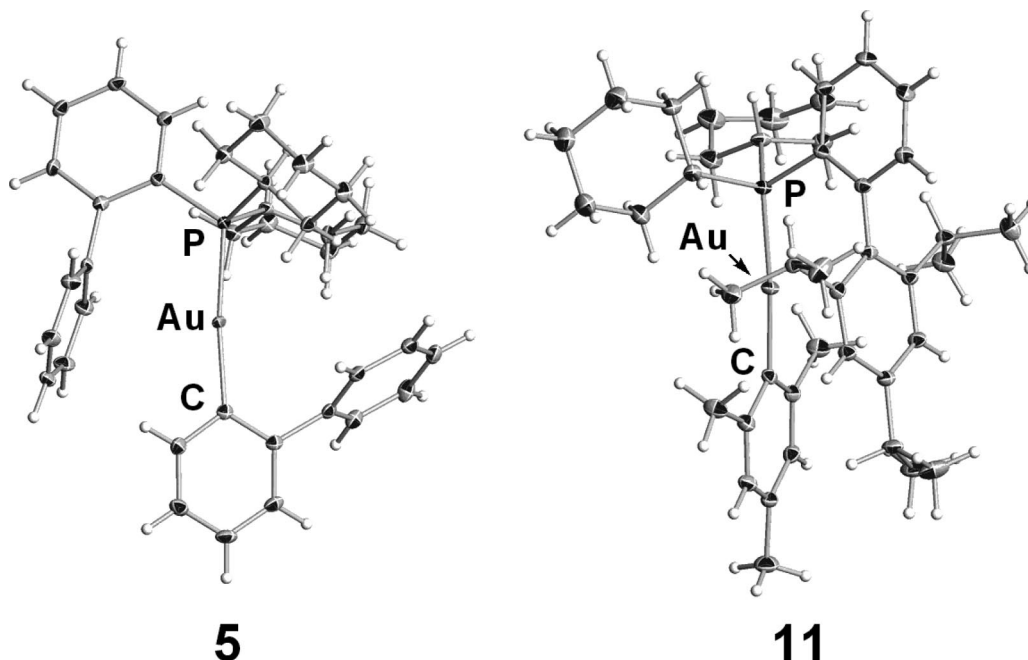
(74) Schmidbaur, H. *Gold Bull.* **2000**, 33, 3–10.

(75) Balch, A. L. *Struct. Bonding (Berlin)* **2007**, 123, 1–40.

(76) Pyykkö, P. *Chem. Rev.* **1997**, 97, 597–636.

(77) Partyka, D. V.; Updegraff, J. B., III; Zeller, M.; Hunter, A. D.; Gray, T. G. *Organometallics* **2007**, 26, 183–186.

(78) Partyka, D. V.; Robilotto, T. J.; Zeller, M.; Hunter, A. D.; Gray, T. G. *Organometallics* **2008**, 27, 28–32.

**Figure 1.** Thermal ellipsoid projections (50% probability, 100 K) of the representative compounds **5** and **11**.**Table 2. Crystallographic Data for Compounds 4–11**

	4	5	6	7	8	9	10	11
formula	C ₃₀ H ₃₆ AuP	C ₃₆ H ₄₀ AuP	C ₃₁ H ₃₈ AuP • 0.83C ₆ H ₆	C ₃₇ H ₄₂ AuP	C ₃₄ H ₄₄ AuP	C ₃₉ H ₅₄ AuP • 1/2C ₅ H ₁₂	C ₄₅ H ₅₈ AuP • 3/4C ₅ H ₁₂	C ₄₂ H ₆₀ AuP
fw	624.52	700.62	645.05	714.64	680.63	786.83	880.96	792.84
cryst syst	monoclinic	monoclinic	triclinic	monoclinic	monoclinic	monoclinic	triclinic	monoclinic
space group	P2 ₁ /n	P2 ₁ /n	P $\bar{1}$	P2 ₁ /n	P2 ₁ /n	P2 ₁ /c	P $\bar{1}$	P2 ₁ /n
<i>a</i> , Å	11.1084(8)	10.9514(7)	12.5163(2)	10.9969(7)	9.8061(2)	10.6912(8)	10.9277(4)	12.5649(1)
<i>b</i> , Å	15.4789(1)	17.0221(1)	12.9094(2)	15.7608(9)	12.7470(2)	15.6268(1)	15.7120(5)	15.9222(1)
<i>c</i> , Å	14.9932(1)	15.5282(1)	26.689(3)	17.9630(1)	23.5452(5)	22.5830(2)	25.4351(9)	19.6846(2)
α , deg			85.599(2)				76.644(2)	
β , deg	94.074(1)	95.918(1)	79.300(2)	100.147(1)	99.527(1)	101.010(1)	87.555(2)	107.572(2)
γ , deg			71.929(2)				87.386(2)	
cell volume, Å ³	2571.5(3)	2879.3(3)	4027.5(8)	3064.6(3)	2902.5(1)	3703.5(5)	4242.3(3)	3754.4(6)
<i>Z</i>	4	4	6	4	4	4	4	4
<i>D</i> _{calcd} , Mg, m ³	1.613	1.616	1.596	1.549	1.558	1.411	1.379	1.403
<i>T</i> , K	100(2)	100(2)	100(2)	100(2)	273(2)	100(2)	173(2)	100(2)
μ , mm ^{−1}	5.799	5.189	5.556	4.876	5.144	4.402	3.537	3.988
<i>F</i> (000)	1240	1400	1929	1432	1368	1612	1814	1624
cryst size, mm ³	0.060 × 0.042 × 0.039	0.65 × 0.49 × 0.48	0.49 × 0.23 × 0.23	0.63 × 0.12 × 0.09	0.31 × 0.10 × 0.05	0.58 × 0.36 × 0.11	0.18 × 0.17 × 0.05	0.57 × 0.51 × 0.29
θ_{\min} , θ_{\max} , deg	1.89, 28.28	1.78, 28.28	0.78, 30.63	1.73, 28.28	4.36, 35.63	1.59, 28.28	1.33, 27.50	1.58, 28.28
no. of reflns collected	26 019	29 650	47 860	31 171	12 907	29 907	67 306	27 825
no. of indep reflns	6373	7073	24 370	7606	10 266	8941	18 752	9038
no. of refined params	289	343	923	353	329	399	903	406
goodness-of-fit on <i>F</i> ²	1.074	1.098	1.011	1.062	1.054	1.063	1.119	1.046
final <i>R</i> indices [<i>I</i> > 2 σ (<i>I</i>)]	0.0183	0.0218	0.0526	0.0196	0.0271	0.0304	0.0566	0.0253
<i>R</i> ₁								
<i>wR</i> ₂	0.0460	0.0560	0.1241	0.0474	0.0544	0.0749	0.1486	0.0633
<i>R</i> indices (all data)	0.0190	0.0229	0.0790	0.0229	0.0440	0.0349	0.0764	0.0290
<i>R</i> ₁								
<i>wR</i> ₂	0.0463	0.0566	0.1365	0.0487	0.0652	0.0772	0.1625	0.0652

Figure 2 depicts absorption spectra of all new compounds in THF. Absorption is confined within the ultraviolet region, with an onset near 325 nm. An absorption shoulder is partly resolved near 275 nm for all compounds.

Absorption spectra of the free phosphine ligands exhibit a broad, featureless transition near 280 nm that resembles the absorption shoulders near the same wavelength in Figure 2. Thus, the absorption shoulders near 280 nm for **4–11** are assigned as a phosphine-based intraligand transition. At higher energies ($\lambda < 275$ nm), absorption in **4–11** increases (not always

Table 3. Selected Interatomic Distances (Å) and Angles (deg) for 4–11

compound	Au–P	Au–C _{ortho}	Au–C _{ipso}	Au–C _{ortho}	\angle P–Au–C _{ortho}
4	2.3048(5)	2.046(2)	3.306(2)	3.246(2)	174.18(6)
5	2.3043(6)	2.060(2)	3.296(2)	3.411(3)	172.18(7)
6	2.2938(15)	2.039(6)	3.313(7)	3.445(7)	169.44(17)
	2.2923(15)	2.048(6)	3.350(6)	3.462(6)	169.13(16)
	2.2981(16)	2.047(7)	3.357(6)	3.273(6)	167.20(19)
7	2.3043(6)	2.060(2)	3.296(2)	3.411(2)	172.18(7)
8	2.2915(6)	2.047(2)	3.195(2)	3.454(2)	172.76(6)
9	2.3033(7)	2.048(3)	3.328(3)	3.225(3)	171.57(10)
10	2.2953(19)	2.022(7)	3.305(6)	3.283(6)	175.85(17)
	2.2911(16)	2.055(6)	3.171(7)	3.366(7)	173.66(19)
11	2.3086(7)	2.065(2)	3.267(2)	3.385(2)	174.78(6)

(84) For a study of *ortho*-substituted biaryl ligands about nickel and rhodium centers, see: Jones, G. D.; Anderson, T. J.; Chang, N.; Brandon, R. J.; Ong, G. L.; Vivic, D. A. *Organometallics* **2004**, *23*, 3071–3074.

monotonically); molar absorptivities exceed 10 000 M^{−1} cm^{−1} at $\lambda = 250$. No such increase is seen for the free phosphines;

Table 4. Hapticities η^x Calculated for Phosphine Biaryl Moieties in the Crystal Structures of 4–11

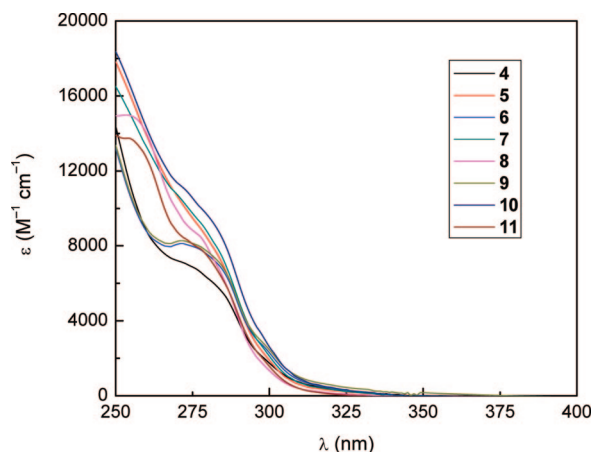
compound	x
4	1.82
5	1.64
6^a	1.73, 1.62, 1.57
7	1.69
8	1.58
9	1.67
10^b	1.41, 1.93
11	1.71

^a Three independent molecules per unit cell. ^b Two independent molecules per unit cell.

Table 5. Close Approaches (Å) of Gold to the Non- σ -bonded Phenyl Ring in Biphenyl Complexes 5, 7, and 10 (all measurements refer to biphenyl ligands σ -bonded to gold)

compound	Au–C _{ipso}	Au–C _{ortho}
5	3.289(2)	3.362(2)
7	3.317(2)	3.225(2)
10^a	3.423(8)	3.269(8)
	3.454(7)	3.336(7)

^a Two independent molecules per unit cell.

**Figure 2.** Room-temperature absorption spectra of new compounds in THF.

molar absorptivities at 250 nm are near 6000 M^{−1} cm^{−1}. The higher-energy optically allowed transitions of 4–11 are expected to have some arylgold(I) character. The orbital origins of these transitions have been investigated with density-functional theory computations. At room temperature and 77 K, 4–11 are nonluminescent.

Computations. Static and time-resolved density-functional calculations were conducted on 4, which is representative of the new arylgold(I) compounds. Compound 5 was also an object of calculations because its σ -bonded *ortho*-biphenyl ligand interacts datively with gold. The geometries are those of the crystal structures, except that hydrogen-atom positions were optimized.

Figure 3 depicts a partial Kohn–Sham orbital energy level diagram. Contributions from the (phosphine)- and (phenyl)gold(I) fragments appear in the figure, as do percentage contributions from Mulliken population analysis.⁸⁵ Implicit THF solvation is incorporated with the polarizable continuum model of Tomasi and co-workers.^{86,87}

For compound 4, the highest-occupied Kohn–Sham orbital (HOMO) is a σ -bonding combination centered between gold and the phenyl-ligand carbon. The gold atom and the σ -bound phenyl carbon atom contribute 67% and 11%, respectively, to this orbital in terms of electron density. The first three lowest

unoccupied Kohn–Sham orbitals (LUMOs) are primarily (>88%) π^* orbitals of the flanking biphenyl group on phosphorus. The calculated HOMO–LUMO gap is 3.30 eV. The frontier orbitals of 5 are analogous, and its HOMO–LUMO gap is 3.32 eV.

A natural bond order (NBO) analysis finds that the gold 5d and 6s orbitals dominate its bonding. There is only a slight participation of the gold 6p orbital in the bonding of 4 or 5 with a maximum occupation number of 0.005e. Similar observations have been made by DeKock,⁸⁸ Schwerdtfeger,⁸⁹ and their respective co-workers. The natural atomic charge of gold is calculated to be 0.255 for 4 and 0.273 for 5. This charge is slightly positive of the mean natural atomic charges of all hydrogens, which are 0.219 for 4 and 0.220 for 5. The charges calculated for the σ -bonded aryl carbons are −0.350 for 4 and −0.329 for 5, just negative of the average charge of all aromatic carbon atoms (−0.217, 4; −0.203, 5). Together these results indicate that the carbon–gold(I) σ -bond is modestly polar, as anticipated by electronegativity arguments. The applicable Pauling electronegativities are 2.4 for gold and 2.55 for carbon.⁹⁰ Plots of the LUMO of the Lewis-acidic (phosphine)gold(I) fragment and the HOMO of the Lewis-basic phenyl anion appear in Figure S6, Supporting Information. These orbitals combine to produce a C–Au bonding combination that is the HOMO of 4 and that carries mainly (phosphine)gold(I) character, cf. Figure 3.

The present calculations do not make an accurate accounting of dispersion and presumably underestimate dative gold-flanking aryl group interactions. The Wiberg bond order in the orthogonalized Löwdin basis⁹¹ between gold and the *ipso* center and the nearer *ortho* carbon in 4 is 0.071 (Au–C_{ipso}) and 0.093 (Au–C_{ortho}); C_{ortho} is nearer gold than C_{ipso} (Table 5). For comparison, the bond order between gold and the bound carbon of the phenyl ligand is 0.975. In *ortho*-biphenyl complex 5, the crystal structure indicates dative interactions between gold and both biphenyl moieties: that bound to phosphorus and that to gold. For the gold-bound biphenyl ligand the Au–C_{ipso} Wiberg bond order (in the Löwdin basis) is 0.064, and for the nearer *ortho* carbon it is 0.082; the *ortho* carbon atom is closer to gold. For the phosphorus-bound biphenyl in the same molecule, the *ipso* carbon is nearer gold than either *ortho* neighbor. The corresponding Wiberg bond orders are nearly the same: 0.074 (Au–C_{ipso}) and 0.075 (Au–C_{ortho}). These results indicate weak carbon–gold interactions in the absence of dispersion.

Time-dependent density-functional theory calculations of the lowest 10 singlet excited states of 4 afford fair agreement with experiment. Table S1, Supporting Information, summarizes the first 10 spin-allowed transitions. The computations find that the absorption shoulder near 280 nm is composed of overlapping optically allowed transitions. Some are nearly pure one-electron promotions, while others are combinations of such transitions intermixing through configuration interaction (CI). Two transitions, calculated at 321.2 and 309.7 nm, bear significant oscillator strength. That at 321.2 nm is 97% composed of a LUMO+1 \leftarrow HOMO−1 promotion. The transition calculated

(85) Mulliken, R. S. *J. Chem. Phys.* **1955**, *23*, 1833–1840.

(86) Miertus, S.; Scrocco, E.; Tomasi, J. *J. Chem. Phys.* **1981**, *55*, 117–129.

(87) Tomasi, J.; Mennucci, B.; Cammi, R. *Chem. Rev.* **2005**, *105*, 2999–3093.

(88) DeKock, R. L.; Baerends, E. J.; Boerrigter, P. M.; Hengelmolen, R. *J. Am. Chem. Soc.* **1984**, *106*, 3387–3396.

(89) Schwerdtfeger, P.; Hermann, H. L.; Schmidbaur, H. *Inorg. Chem.* **2003**, *42*, 1334–1342.

(90) Allred, A. L. *J. Inorg. Nucl. Chem.* **1961**, *17*, 215–221.

(91) Wiberg, K. B. *Tetrahedron* **1968**, *24*, 1083–1096.

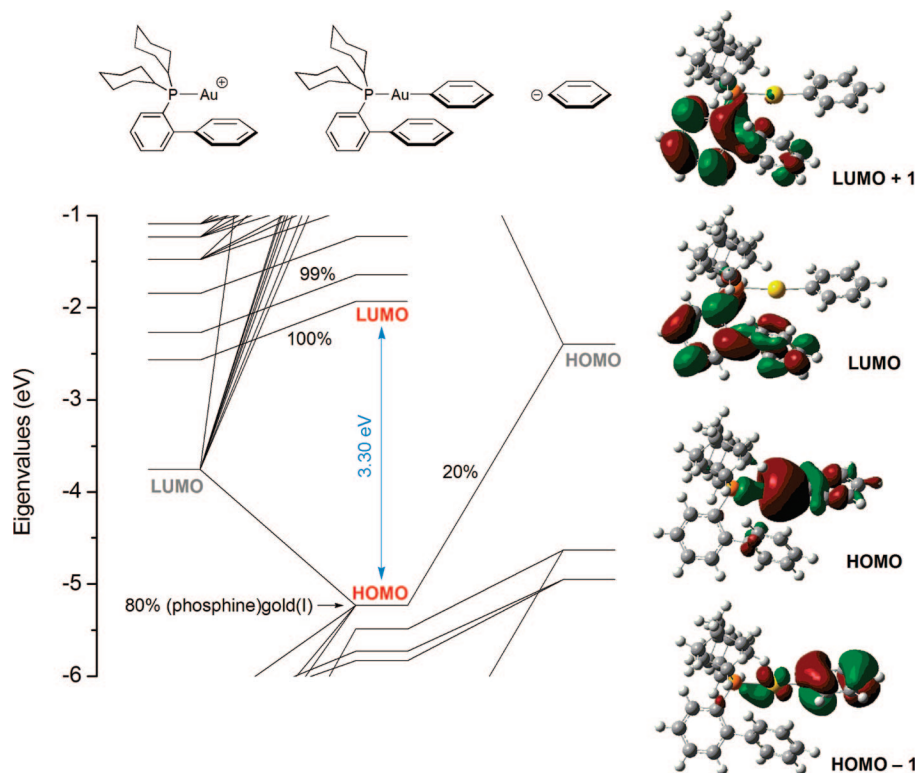


Figure 3. Kohn–Sham orbital correlation diagram for **4**. Fragments are the (phosphine)gold(I) fragment (left) and the phenyl ligand, right (mpwpw91/Stuttgart ECP and basis on Au; TZVP on nonmetal atoms); implicit THF solvation is included through a polarizable continuum model. Right: plots of selected orbitals (contour level 0.03 au).

at 309.7 nm is primarily composed of four one-electron excitations that undergo configuration interaction: LUMO \leftarrow HOMO–3 (60%), LUMO \leftarrow HOMO–2 (16%), LUMO \leftarrow HOMO–4 (11%), and LUMO+1 \leftarrow HOMO–2 (6%). Both the LUMO and LUMO+1 are localized on the phosphine biaryl substituent, as plotted in Figure 3, right. Diagrams of the HOMOs–2, 3, and 4 appear in Figure S1, Supporting Information. The HOMO–3 and HOMO–2 have extensive phenyl-ligand π -character that derives from an e_g orbital of free benzene. The HOMO–4 has little phenyl-ligand character and is primarily concentrated on gold and the phosphine ligand.

It is notable that no singlet–singlet transition involving the C–Au σ -bond (i.e., the HOMO) carries substantial oscillator strength. For example, the lowest-lying singlet excited state is calculated at 373.4 nm; it consists (99%) of a LUMO \leftarrow HOMO excitation. Similarly, the LUMO+1 \leftarrow HOMO promotion (97%) affords the third singlet excited state, calculated at 343.1 nm. The more intense of these transitions originating from the HOMO has but 6.0% the oscillator strength of the intense transition calculated at 309.7 nm. That is, the carbon–gold bond is essentially nonchromophoric.

Conclusions

Aryl-group transfer from boron reagents has previously been shown to tolerate reducible and polar functionalities in aryl-gold(I) complex synthesis.⁵³ The dicyclohexylbiarylphosphines first popularized by Buchwald and co-workers^{36–49} were chosen as sterically encumbering ancillary ligands. Compounds bearing simultaneous bulk at the phosphorus center and in the σ -aryl ligand are preparable in isolated yields ranging from 45 to 90%. Further, arylation from boron avoids pyrophoric reactants such as aryllithium compounds and Grignard reagents. The new compounds are indefinitely stable as solids to air, moisture, and laboratory lighting.

Crystallographic characterization reveals dative interactions between gold and the flanking biaryl groups bound to the phosphine ligands. In most compounds, the primary attractive interaction is between the phosphine *ipso* carbon and gold, although in a few structures, an *ortho* carbon has a closer approach to gold. Kochi hapticities for 11 crystallographically independent structures in eight distinct compounds are in the range 1.41–1.93. Further, dative interactions prevail in three gold complexes bearing σ -bonded *ortho*-biphenyl ligands (compounds **5**, **7**, and **10**). In these, the *ipso* and one *ortho* carbon of the non- σ -bonded phenyl ring interact in a sidewise manner with gold. Clearly, the proclivity of gold(I) to adopt two-coordinate structures does not exclude higher coordination numbers through π -interaction with available aromatic donors. This finding concurs with recent demonstrations of tricoordinate gold(I)^{92–96} and with an established tendency of linear gold(I) to undergo associative ligand substitutions.^{97–100}

Excited-state properties of dialkylbiarylphosphine metal complexes are also reported, apparently for the first time. The new compounds, which are white or pale yellow as solids, absorb in the ultraviolet region, with absorption onsets near 350 nm in THF. Absorption features near 280 nm are visible in the spectra of all complexes. Time-dependent density-functional calculations on the representative complexes **4** and **5** indicate these to be (ligand–metal)-to-ligand charge-transfer transitions

(92) Teets, T. S.; Partyka, D. V.; Esswein, A. J.; Updegraff, J. B. III; Zeller, M.; Hunter, A. D.; Gray, T. G. *Inorg. Chem.* **2007**, *46*, 6218–6220.

(93) Meiners, J.; Herrmann, J.-S.; Roesky, P. W. *Inorg. Chem.* **2007**, *46*, 4599–4604.

(94) Esswein, A. J.; Dempsey, J. L.; Nocera, D. G. *Inorg. Chem.* **2007**, *46*, 2362–2364.

(95) Assefa, Z.; Forward, J. M.; Grant, T. A.; Staples, R. J.; Hanson, B. E.; Mohamed, A. A.; Fackler, J. P., Jr. *Inorg. Chim. Acta* **2003**, *352*, 31–45.

(96) Gimeno, M. C.; Laguna, A. *Chem. Rev.* **1997**, *97*, 511–522.

between the arylgold(I) fragment and the biarylphosphine ligand. The same computations find the carbon–gold σ -bond to be nonchromophoric. Static DFT calculations indicate a weakly polar C–Au bond, as expected from the small difference in their Pauling electronegativities.

Acknowledgment. The authors thank the National Science Foundation (grant CHE-0749086 to T.G.G.) and Case

Western Reserve University for support. The diffractometer at CWRU was funded by NSF grant CHE0541766; that at YSU by NSF grant 0087210, by the Ohio Board of Regents grant CAP-491, and by Youngstown State University. We thank Mr. Thomas Teets, Massachusetts Institute of Technology, for experimental assistance and Professor D. G. Nocera, MIT, for access to instrumentation.

Supporting Information Available: Thermal ellipsoid projections of **6**, **7**, **8**, and **10**; plots of selected orbitals of **4**, first 10 calculated singlet–singlet transitions of **4**; full citation of ref 54, and crystallographic (CIF) data. This material is available free of charge via the Internet at <http://pubs.acs.org>.

OM800746U

(97) Dickson, P. N.; Wehrli, A.; Geier, G. *Inorg. Chem.* **1988**, 27, 2921–2925.

(98) Boles-Bryan, D. L.; Mikuriya, Y.; Hempel, J. C.; Mellinger, D.; Hashim, M.; Pasternack, R. F. *Inorg. Chem.* **1987**, 26, 4180–4185.

(99) Schmidbaur, H.; Shiotani, A.; Klein, H.-F. *Chem. Ber.* **1971**, 104, 2831–2837.

(100) Isab, A. A.; Sadler, P. J. *J. Chem. Soc., Dalton Trans.* **1982**, 135–141.